0026-895X/90/040535-11$02.00/0

MOLECULAR PHARMACOLOGY, 37:535-545

Non-Steady State Kinetic Analysis of the Regulation of Adenylate Cyclase by GTP-Binding Proteins

J. D. BELL, R. L. BILTONEN, and L. L. BRUNTON

Departments of Pharmacology and Biochemistry, University of Virginia School of Medicine, Charlottesville, Virginia 22908 (J.D.B., R.L.B.) and Department of Pharmacology, University of California, San Diego, La Jolla, California 92093 (L.L.B.)

Received May 23, 1989; Accepted December 22, 1989

SUMMARY

The time course of cAMP production by S49 cell membranes in the presence of forskolin and a nonhydrolyzable GTP analog can yield information about the regulation of adenylate cyclase by both the inhibitory and stimulatory GTP-binding proteins (G_i and G_s). The time courses are complex and interpretation in terms of the activities of G_i and G_s requires a quantitative hypothesis. We present a general quantitative hypothesis that defines adenylate cyclase as existing in a distribution of two states, active and inactive. G_i and G_s, in their active states, alter the equilibrium of this distribution. Two distinct models are derived based on this hypothesis to accommodate two different proposed mechanisms for the action of G_i to inhibit adenylate cyclase: 1) a direct interaction between G_i and the catalytic subunit of adenylate cyclase and 2) a direct interaction between G_i and G_s. Perturbations of the regulation of adenylate cyclase by pertussis toxin and phorbol ester are simulated and interpreted using the models. The effect of pertussis toxin is quantitatively reconciled by decreases in the guanine nucleotide-independent adenylate cyclase activity and in the apparent rate of activation of G_i from 2.0/min to 0.01/min. The effect of phorbol ester is best accommodated by the model as a change in the distribution of active and inactive adenylate cyclase from 36% initially active to 47% active after phorbol ester treatment, without postulating any effect of phorbol ester on G_i or G_s. Both of these interpretations are independent of the model used. The effect of forskolin is also examined within the context of the two models. The results of this examination suggest an experimental approach for testing the models. These examples illustrate the usefulness of quantitative analysis of time course data using a model for the regulation of adenylate cyclase. We propose that, with this combined experimental and theoretical approach, one can address the relevance of hypotheses generated from experimental studies with isolated components to the molecular mechanisms of adenylate cyclase regulation in cellular membranes.

A minimum of three protein components are required to reconstitute dual-regulated adenylate cyclase (1). The catalytic subunit is a M_r 150,000 transmembrane glycoprotein that can be activated by the diterpene forskolin. Two GTP-binding proteins modulate adenylate cyclase activity either positively (G_s) or negatively (G_i). Apparently, these GTP-binding proteins functionally couple hormone receptors to the catalytic subunit, providing a mechanism for both stimulatory and inhibitory regulation of adenylate cyclase. Both GTP-binding proteins are heterotrimers, consisting of α subunits (M_r 45,000–46,000 for G_s and ~41,000 for G_i), β subunits (M_r ~ 35,000), and γ subunits (M_r ~8,000). The accepted mechanism for stimulation of adenylate cyclase by G_s states that G_s dissociates in the presence of Mg^{2+}GTP and that the α subunit binds to the catalytic subunit, promoting increased activity. The α subunit possesses intrinsic GTPase activity. Upon hydrolysis of the bound GTP, the α subunit-GDP complex reassociates with the β and γ subunits, returning G_s to the inactive state. The steady state concentration of active G_s is dictated by the rate of GDP/GTP exchange, which is catalyzed by the hormone receptor in the presence of receptor agonists. In the absence of receptor agonist, G_s is persistently, but slowly, activated by nonhydrolyzable GTP analogs.

G_i is apparently activated in a manner analogous to G_s. However, it is less clear how G_i inhibits adenylate cyclase activity. Some evidence has suggested that either the α subunit (2, 3) or the β subunit (4, 5) of G_i may directly bind to the catalytic subunit and inhibit it. In contrast, evidence from reconstitution studies suggests that active G_i decreases the concentration of active G_s by the law of mass action (1, 6; 7). The β and γ subunits of both G_s and G_i are interchangeable if not identical (1). Dissociation of G_i would increase the free concentration of β/γ subunits in the membrane and these would

This work was supported by Grants DCB8600086 of the National Science Foundation and DK07320, GM07267, and GM11838 from the National Institutes of Health and by a predoctoral fellowship to J.D.B. from the Pharmaceutical Manufacturers Association Foundation.

ABBREVIATIONS: G_s, stimulatory GTP-binding transducer protein; G_i, inhibitory GTP-binding transducer protein; TPA, 12-*O*-tetradecanoylphorbol-13-acetate; HEPES, 4-(2-hydroxyethyl)-1-piperazineethanesulfonic acid; EGTA, [ethylenebis(oxyethylenenitrilo)]tetraacetic acid; Gpp(NH)p, guanosine (5′-(β,γ-imino)triphosphate.

shift the position of the equilibrium of G_s toward its associated inactive state.

The difficult experimental question from reconstitution studies is assessing their relevance to *in situ* systems. One must test the information obtained from purified systems in native membranes and eventually in intact cells. This, of course, becomes increasingly difficult as one moves to more complex systems. Several years ago, Hudson and Fain (8) demonstrated that, under certain experimental conditions, one can observe both time-dependent inhibition and stimulation of adenylate cyclase by a nonhydrolyzable GTP analog in a single time course. At that time, little was known about the GTP-binding proteins, and the various current hypotheses of adenylate cyclase regulation had not yet been articulated. However, given the subsequent progress in the understanding of adenylate cyclase components, the time courses reported by Hudson and Fain suggest a promising experimental system for assessing in cell membranes the relevance of specific hypotheses generated from reconstitution studies. Meaningful interpretation of these non-steady state time courses requires a quantitative model of the hypothesis being tested.

We have formulated a quantitative model for interpretation of time courses of dual regulation of adenylate cyclase activity by a nonhydrolyzable GTP analog and we show how this model can be transformed to accommodate certain specific molecular hypotheses. Computer simulations of such time courses provide information into how variation of specific molecular parameters alters the shape of the time courses. The simulated data allow quantitative comparison of specific hypotheses and provide insight into the design of future experiments to distinguish those hypotheses. For example, it has become clear from the simulations in this study that knowledge of the state of the system before activation by guanine nucleotides may be the singularly most important piece of information required to distinguish between hypotheses for the mechanism of adenylate cyclase inhibition. Of particular importance, these simulations also demonstrate that simple visual interpretation of experimental time courses can lead to erroneous interpretations. For example, it is shown that changes in the "lag time" of a product-time profile by an experimental perturbation does not necessarily mean that rates of activation of the GTP-binding proteins have been altered.

We use the general model to examine specific experimental perturbations of the system. First, we show that the model is consistent with a previous hypothesis concerning the functional effect of pertussis toxin on adenylate cyclase. Second, we investigate the use of the model to ask a specific question about a less understood perturbant of adenylate cyclase regulation, phorbol ester. Finally, we evaluate the qualitative features of the effect of forskolin on adenylate cyclase activity and establish conditions that are necessary to rationalize existing data in terms of the two proposed mechanisms of G_i-mediated inhibition. This evaluation suggests a specific experimental design for obtaining important quantitative information about the initial state of the system (before modulation by guanine nucleotides) to investigate the possible mechanisms of inhibition by G_i in cellular membranes.

Experimental Procedures

S49 cells and membranes. S49 cells were grown as previously described (9, 10). For experiments involving treatments of intact cells with the phorbol ester TPA, cells were collected by centrifugation, washed once in growth medium without serum, suspended at a density of approximately 10^7/ml in growth medium without serum, and incubated for 10 min at 3°. TPA (100 nM) or equivalent diluent (ethanol) was then added and the incubation was continued an additional 10 min. When experiments required 24-hr incubations with pertussis toxin *in vivo*, cells were suspended at a density of about 10^6/ml in growth medium with 6% horse serum. Pertussis toxin was added to half of the cells at a final concentration of 100 μg/ml; the remainder of the cells served as the control. The cells were then incubated under the standard cell culture conditions for about 24 hr.

Adenylate cyclase assays. Cells were collected by centrifugation following the various treatments described above, and membranes were prepared by a freeze-thaw procedure described previously (9). Protein content was determined by the method of Bradford (11). Adenylate cyclase activity was assessed in membrane preparations using the method of Salomon *et al.* (12).

Reactions were initiated by the addition of membranes (about 50–200 μg of protein) to a reaction mixture (850–950 μl final volume) containing 50 mM Na^+ HEPES (pH 7.5), 1 mM [α-^{32}P]ATP (20–50 cpm/pmol), 2 mM $MgCl_2$, 0.2 mM isobutyl methylxanthine, 0.1 mg/ml bovine serum albumin, 0.4 mM EGTA, and 50 μM forskolin. For cyc$^-$ S49 cell membranes, the reaction mixture was identical except that the specific activity of the [α-^{32}P]ATP was 70–180 cpm/pmol, 0.1 mM $MnCl_2$ replaced the $MgCl_2$, and no EGTA was included. Gpp(NH)p was included as specified in the individual experiments. The membranes were incubated for several minutes at the reaction temperature (27°) before initiation of assays. Reactions were terminated at the indicated times by diluting 100-μl aliquots (5–20 μg of membrane protein) into stop solution (12), and the [^{32}P]cAMP was purified as described (12). The profiles of the time courses obtained in these experiments are extremely sensitive to the concentration of forskolin, Gpp(NH)p, and free $MgCl_2$, as described previously (8, 10). Therefore, the concentrations of reagents in the reaction mixture were carefully chosen to obtain measurable inhibitory and stimulatory phases in the time courses. It should be noted that we have ignored the short latency in the onset of forskolin-stimulated adenylate cyclase activity (13) in our analysis. The experimental manipulation of incubating the membranes with forskolin before the addition of Gpp(NH)p assures linear time courses in the absence of guanine nucleotide but also greatly attenuates the biphasic nature of the time course obtained with Gpp(NH)p. In this study, the forskolin latency was very short relative to the resolution of the time courses and frequently nonexistent. Therefore, we made the simplifying assumption in the simulations that the time courses of forskolin-stimulated cAMP generation were linear from time zero. In the experimental data, any possible biasing effects of the latency in forskolin stimulation were compensated, because the data were normalized to that obtained in the presence of forskolin alone (see legends to Figs. 1, 5, and 6).

Computer simulations and statistics. The differential equations describing the models were numerically integrated by computer using Simpson's rule. The integration interval was 0.01 min. The degree of agreement between experimental data and the computer simulations was judged by calculating the sum of the squares of the residuals between the simulated data and the pooled experimental data.

Model

We assume that the modulation of cAMP production by the nonhydrolyzable guanine nucleotide Gpp(NH)p can be described by the interactions of three protein components, G_s, G_i, and the catalytic subunit of adenylate cyclase. Each component is assumed to exist in one of two states, i.e., active or inactive. The production of cAMP by the entire system as a function of time reflects time-dependent changes in the distribution of active and inactive states of each component. The relative proportion of active and inactive catalytic subunit (A_1 and A_0, respectively) in the absence of activated GTP-binding proteins is defined by the equilibrium constant K_a.

$$A_0 \overset{K_o}{\rightleftharpoons} A_1$$

In the absence of any activators or inhibitors (e.g., forskolin or activated GTP-binding protein), the system would be in its true basal state and presumably only a small proportion of the catalytic subunit would be in state A_1. It is assumed that any perturbation such as forskolin or the GTP-binding proteins stimulates or inhibits the system by either directly or indirectly altering the equilibrium proportion of active and inactive catalytic subunits. The coupling of all modulators is via this reversible equilibrium between A_1 and A_0. Under no condition (other than at absolute zero) does the enzyme exist entirely in either state. The adenylate cyclase activity (dcAMP/dt) is a function of the apparent turnover number (k_c) and the concentration of catalytic subunit (A_T) weighted by the proportion of catalyst in the active state.

$$\frac{d\text{cAMP}}{dt} = \frac{k_c A_T \Sigma A_{1_j}}{\Sigma A_{0_j} + \Sigma A_{1_j}} \tag{1}$$

where j refers to the individual species of A_1 or A_0.

Various hypotheses concerning the mechanism of modulation of catalytic activity by the GTP-binding proteins G_s and G_i are incorporated into the general model by defining the interaction of these proteins with each other and with the two states of the catalytic subunit. We consider two specific models for these interactions.

In model I, it is assumed that the active states of G_s and G_i (G_s* and G_i*) interact directly with A_1 and A_0 and that equilibrium is rapidly achieved.

$$A_0G_i^* \overset{K_i}{\rightleftharpoons} G_i^* + A_0 \overset{K_o}{\rightleftharpoons} A_1 + G_s^* \overset{K_s}{\rightleftharpoons} A_1G_s^*$$

In this model, $\Sigma A_{1_j} = A_1 + A_1G_s^*$ and $\Sigma A_{0_j} = A_0 + A_0G_i^*$. The rate of cAMP production is, therefore, given by

$$\frac{d\text{cAMP}}{dt} = \frac{k_c A_T K_o(1 + K_sG_s^*)}{1 + K_iG_i^* + K_o(1 + K_sG_s^*)} \tag{2}$$

No direct interaction between G_s* and G_i* is assumed in this model. The time dependence for the accumulation of G_s* and G_i* is defined by the following relationships.

$$G_s^* = G_{s_0}^* + G_{s_0}(1 - e^{-k_s t}) \tag{3}$$

$$G_i^* = G_{i_0}^* + G_{i_0}(1 - e^{-k_i t}) \tag{4}$$

G_{s_0}* and G_{i_0}* are the concentrations of G_s and G_i that are active at time zero. G_{s_0} and G_{i_0} are the maximum concentrations of G_s and G_i that can become activated in the presence of Gpp(NH)p with apparent rate constants k_s and k_i. Substituting Eqs. 3 and 4 into Eq. 2 gives

$$\frac{d\text{cAMP}}{dt} = \frac{k_c A_T K_o[1 + K_sG_{s_0}^* + K_sG_{s_0}(1 - e^{-k_s t})]}{1 + K_iG_{i_0}^* + K_iG_{i_0}(1 - e^{-k_i t}) + K_o[1 + K_sG_{s_0}^* + K_sG_{s_0}(1 - e^{-k_s t})]} \tag{5}$$

In making these substitutions, we assume that the concentrations of G_s* and G_i* are not significantly depleted by interactions with A_1 and A_0, which seems reasonable based on experimental data indicating a substantial excess of G_s and G_i over the catalytic subunit in native tissue (1). The assumption of rapid equilibria for K_s, K_i, and K_0 also appears consistent with experimental results (14, 15). In molecular terms, G_s* represents the α subunit of G_s, and G_i* could represent either the α or β subunit of G_i, depending on the experimental system or hypothesis being investigated (1–5).

Model II assumes no direct interaction between G_i* and A_0 but rather that G_i* binds to G_s*, preventing its interaction with A_1.

$$\begin{array}{ccccc} & & A_0 & & \\ & & \Downarrow K_o & & \\ A_1G_s^* & \overset{K_s}{\rightleftharpoons} & A_1 + G_s^* + G_i^* & \overset{K_{i_2}}{\rightleftharpoons} & G_i^*G_s^* \end{array}$$

For this case, G_s* represents the α subunit of G_s and G_i* is the β subunit of G_i (6, 7). Because no direct interaction between G_i* and A_0 is assumed, $\Sigma A_{0_j} = A_0$ and Eq. 2 becomes

$$\frac{d\text{cAMP}}{dt} = \frac{k_c A_T K_o(1 + K_sG_s^*)}{1 + K_o(1 + K_sG_s^*)} \tag{6}$$

If $G_i \gg G_s$*, then

$$G_s^* = \frac{G_{s_0}^* + G_{s_0}(1 - e^{-k_s t})}{1 + K_iG_{i_0}^* + K_iG_{i_0}(1 - e^{-k_i t})} \tag{7}$$

If, however, G_i* is not significantly greater than G_s*, then

$$G_i^* = \frac{G_{i_0}^* + G_{i_0}(1 - e^{-k_i t})}{1 + K_iG_s^*} \tag{8}$$

and

$$G_s^* = \frac{\sqrt{b^2 + 4K_ic} - b}{2K_i} \tag{9}$$

where

$$b = 1 + K_i[G_{i_0}^* + G_{i_0}(1 - e^{-k_i t}) - G_{s_0}^* - G_{s_0}(1 - e^{-k_s t})] \tag{10}$$

$$c = G_{s_0}^* + G_{s_0}(1 - e^{-k_s t}) \tag{11}$$

These two models demonstrate how the general model described by Eq. 2 can be altered to accommodate two different hypotheses for the molecular details of adenylate cyclase regulation. Other hypotheses that have been proposed, such as the possibility that G_s and the catalytic subunit are always physically coupled (16), can also be readily incorporated into the general model represented by Eq. 2.

Results and Discussion

Comparison of experimental and simulated time courses. Experimentally, cAMP production was a linear function of time in the presence of 50 μM forskolin with no added guanine nucleotide, in S49 cell membranes at 27°. This is defined as the experimental reference condition and is the experimental equivalent of the initial state in the models before GTP-binding protein activation. For comparison of experimental data with the computer simulations, the slope of this line was assigned a value of 1.0 unit/min and all experimental data were normalized to this reference (Fig. 1A). In the presence of both forskolin and the nonhydrolyzable GTP analog Gpp(NH)p (10 μM), the time course of cAMP production was more complex (Fig. 1A); the rates at early times were clearly less when Gpp(NH)p was included than with forskolin alone. At long times, the activity was greater with forskolin plus Gpp(NH)p than with forskolin alone.

We verified that the curve in Fig. 1A for forskolin plus Gpp(NH)p is different from a straight line by the following criteria. For each individual experiment of those pooled in Fig. 1A, we found that the data were better fit by a second-order polynomial than by a straight line, according to an F test. The probability that the data are curved according to that procedure was greater than 0.99 for all six experiments. Whether they all had the same curvature was judged by examining the variability of the second-order coefficient among the six experiments and by testing whether the value was equal to 0 by Student's t test. The value of the coefficient was 1.41×10^{-2}, ± a SD of 6.55×10^{-3}. The probability of this coefficient equalling 0 was 0.0033. In the case of the reference line [no Gpp(NH)p], the linear fit could not be distinguished from a polynomial fit based on the F test.

The data of Fig. 1 can be quantitatively simulated by numer-

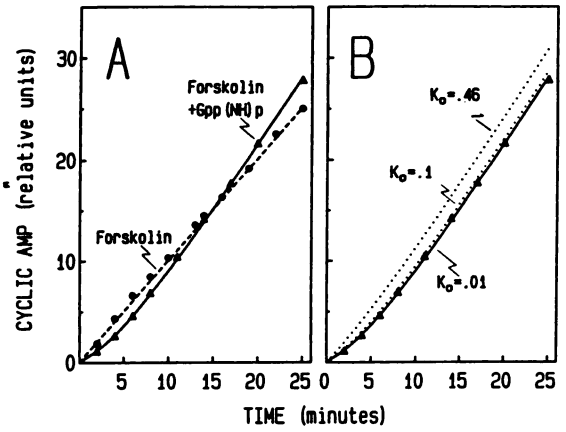

Fig. 1. Comparison of experimental and theoretical time courses of forskolin-stimulated cAMP production modulated by Gpp(NH)p. A, S49 cell membranes were assayed for adenylate cyclase activity in the presence of 50 μM forskolin without (●) or with (▲) 10 μM Gpp(NH)p, as described in Experimental Procedures. Data are the mean of six experiments (the three control experiments each from Figs. 5 and 6) normalized to the adenylate cyclase activity measured with forskolin alone (314 ± 39 pmol/min/mg of protein at 2-min point; all other points, 349 ± 52 pmol/min/mg of protein) (– – –). Consequently, the data are expressed in relative units with 1 unit = amount of cAMP produced at 27° in the presence of 50 μM forskolin and the rest of the reaction cocktail, in the absence of Gpp(NH)p, with 1 mg of membrane protein in 1 min. Theoretical curves were generated by numerical integration of Eq. 5. – – –, Simulation of the effects of forskolin: k_cA_T = 2.8 units/min, K_o = 0.56, $K_iG_{i_0}{}^*$ = 1.0, $K_sG_{s_0}{}^*$ = 1.0, $K_iG_{i_0}$ = 0, and $K_sG_{s_0}$ = 0. ——, Simulation of the effect of Gpp(NH)p: k_cA_T = 2.8 units/min, k_i = 2.0/min, k_s = 0.14/min, K_o = 0.56, $K_iG_{i_0}$ = 1.0, $K_sG_{s_0}{}^*$ = 1.0, $K_iG_{i_0}$ = 9.36, and $K_sG_{s_0}$ = 16.71. B. ▲ and ——, same as for A. · · · ·, generated using Eqs. 6 and 7 (model II) with k_cA_T, k_i, and k_s the same as in A. K_o was varied (0.46, 0.1, and 0.01; *upper* to *lower curves*), $K_iG_{i_0}{}^*$ was arbitrarily selected, and $K_sG_{s_0}{}^*$, $K_iG_{i_0}$, and $K_sG_{s_0}$ were calculated analogously to Eqs. 12–15 with λ_1–λ_4 identical to those used for calculation of the parameters of A (*upper* to *lower curves*, respectively, 0.1, 0.24, 10.36, and 11.22; 0.4, 6.44, 7.4, and 65.7; and 1.0, 110, 9.52, and 938). The *latter curve* superimposes the *solid curve*.

ical integration of Eq. 5 (model I), assigning appropriate values to the constants as follows. Four rates of cAMP formation, estimated from the experimental time courses, are described by the following set of equations.

$$\lambda_1 = \frac{(k_cA_T)\alpha}{1+\alpha} \tag{12a}$$

$$\lambda_2 = \frac{(k_cA_T)(\alpha+\beta)}{1+\alpha+\beta+\gamma} \tag{12b}$$

$$\lambda_3 = \frac{(k_cA_T)\alpha}{1+\alpha+\gamma} \tag{12c}$$

$$\lambda_4 = \frac{(k_cA_T)(\alpha+\beta)}{1+\alpha+\beta} \tag{12d}$$

The terms 1, α, β, and γ denote, respectively, the statistical weight of all species of A_0 at $t = 0$ (statistical weight of 1), all A_1 at $t = 0$ (α), additional A_1 produced with Gpp(NH)p (β), and additional A_0 produced with Gpp(NH)p (γ). λ_1, the rate of cAMP production in the absence of Gpp(NH)p (the reference state) is, by definition, 1.0 unit/min. λ_2 is the rate when both G_s and G_i are maximally activated ($t = \infty$). λ_2 was estimated from the experimental maximum rate of cAMP production in the presence of Gpp(NH)p (Fig. 1) to be greater than or equal to 1.3 units/min. λ_3 corresponds to the rate measured when only G_i is activated by Gpp(NH)p. λ_3 was estimated from the initial time point of the time course of cAMP production in the presence Gpp(NH)p (Fig 1) to be less than 0.5 units/min. λ_4 denotes the condition when only G_s has been activated by Gpp(NH)p and could not be directly determined from the data of Fig. 1A. However, because γ must be positive, λ_4 must be greater than or equal to λ_2. At the high concentrations of Gpp(NH)p and forskolin used in these experiments (10 and 50 μM, respectively), it was reasonable to estimate that the adenylate cyclase would be at least 80–90% active in the absence of G_i. The maximum adenylate cyclase activity obtained after pertussis toxin treatment (see Fig. 5) indicated that λ_4 is about 84% of k_cA_T, as will be discussed.

Values for k_cA_T, α, β, and γ were calculated by simultaneous solution of Eqs. 12a–d, using the initial estimates of λ_1, λ_2, λ_3, and λ_4. The constants for Eq. 5 were then calculated directly using the following relationships:

$$K_sG_{s_0}{}^* = \frac{\lambda_1(1+K_iG_{i_0}{}^*+K_o)-k_cA_TK_o}{K_o(k_cA_T-\lambda_1)} \tag{13}$$

$$K_sG_{s_0} = \frac{\lambda_4[1+K_iG_{i_0}{}^*+K_o(1+K_sG_{s_0}{}^*)]-k_cA_TK_o(1+K_sG_{s_0}{}^*)}{K_o(k_cA_T-\lambda_4)} \tag{14}$$

$$K_iG_{i_0} = \frac{(k_cA_T-\lambda_2)[K_o(1+K_sG_{s_0}{}^*+K_sG_{s_0})]}{\lambda_2} - (1+K_iG_{i_0}{}^*) \tag{15}$$

Because the initial concentrations of G_s* and G_i* were not known experimentally, we selected arbitrary values for $K_iG_{i_0}{}^*$ and K_o. For each set of values for $K_iG_{i_0}{}^*$ and K_o, a set of exact values for $K_sG_{s_0}$, and $K_iG_{i_0}$ were obtained.

The numerical values for the apparent rate constants were determined by first assigning k_i equal to 2.0/min [consistent with the rapid inhibition of forskolin-stimulated adenylate cyclase activity in the presence of 10 μM Gpp(NH)p (see Fig. 1A and Ref. 10)]. Based on the shape of the time course in the presence of Gpp(NH)p (Fig. 1), k_s must be less than k_i and on the order of 0.1/min. The values for k_s, λ_2, λ_3, and λ_4 were then optimized by iterative simulations of the experimental time courses, using Eqs. 5 and 12–15. The optimum values for λ_2, λ_3, and λ_4 were found to be 1.34, 0.25, and 2.35 units/min, respectively. As shown by the *solid curve* in Fig. 1A, the simulated time course agrees well with the experimental data.

As stated above, a unique solution for all the constants of Eq. 5 cannot be obtained with these experimental data. However, regardless of the arbitrary values selected for K_o and $K_iG_{i_0}{}^*$, the numerical integration of Eq. 5 always produces the same time course when the remaining constants are calculated as described above. This means that, for model I, the relative initial proportions of A_1G_s*, A_1, A_0, and A_0G_i* are not important as long as the appropriate ratio of all A_1 species to all A_0 species is maintained (i.e., the condition of λ_1 = 1.0 unit/min is satisfied). All simulations of data in this study with model I will use K_o = 0.56, unless otherwise stated.

In contrast, the simulated time course of cAMP production using model II (Eqs. 6–11, in which G_i and G_s* directly interact) are very dependent on the selection of initial conditions describing A_1 and A_1G_s*. For example, in the simulation of the data presented in Fig. 1A, the fraction of the enzyme in states

A_1 and $A_1G_s^*$ was 0.36 with 50 μM forskolin alone. Consider a few possible distributions of that fraction:

1) $A_1 = 0.36$ $A_1G_s^* = 0.0$

2) $A_1 = 0.18$ $A_1G_s^* = 0.18$

3) $A_1 = 0.0$ $A_1G_s^* = 0.36$

Because inhibition in model II occurs only through the interaction of G_i^* with G_s^*, it is obvious that distribution 1 cannot be inhibited by G_i^* during the early portion of the time course before significant G_s activation. Distribution 3 would be the most sensitive to initial inhibition by G_i^* in model II. This point is illustrated graphically in Fig. 1B. The *dotted curves* in Fig. 1B represent simulations of Eqs. 6 and 7, using constants calculated by a procedure analogous to that described above (Eqs. 13–15) for various values of K_o and $K_{i_s}G_{i_0}^*$ and using the same values of λ_1, λ_2, λ_3, λ_4, k_cA_t, k_i, and k_s as for model I. A different time course was obtained for each selected value of K_o (each representing a different distribution of A_1 and $A_1G_s^*$). However, for any given value of K_o, the resulting time course was insensitive to the choice of $K_{i_s}G_{i_0}^*$ when the remaining parameters were calculated similarly to the procedure described for model I. The experimental data were best reproduced by the simulations at the lowest value of K_o (Fig. 1B, *solid curve*) and this value (0.01) will be used in all simulations of model II in this study.

The important experimental distinction between the two hypotheses for the inhibition of adenylate cyclase by G_i is found in the conditions that exist before the addition of guanine nucleotides to the system (i.e., the reference state). If the proportions of adenylate cyclase in states A_1 and $A_1G_s^*$ at time zero could be determined, the viability of model II could be quantitatively tested. This point will be examined in detail below in the discussion of the effects of forskolin on adenylate cyclase activity.

Effects of perturbations to the model. The sensitivity of the models to changes in the apparent rate constants k_s and k_i is demonstrated in Fig. 2. When k_s equals 0, the time course has a decreasing slope. When k_i equals 0, the slope of the time course is always increasing. The time course contains an inflection point when both k_i *and* k_s are nonzero. The slope increases then decreases if $k_s > k_i$, and it decreases then increases when $k_i > k_s$. With model I, the time courses obtained with perturbations of k_i and k_s are independent of the initial conditions (i.e., the value of K_o and $K_iG_{i_0}$) as long as the appropriate ratio of active to inactive adenylate cyclase is maintained (i.e., $\lambda_1 = 1.0$ unit).

In contradistinction to the effect of perturbation of the rate constants, the time courses obtained upon perturbing the equilibrium constants K_i and K_s depend on the choice of initial conditions. Fig. 3 shows the effect of variation of K_i and K_s upon the simulated time course. The *dashed* and *dotted lines* represent the same perturbation of K_i or K_s at alternative values for $K_iG_{i_0}^*$, at constant K_o. Experimental perturbations of time courses of cAMP production in the presence of Gpp(NH)p and forskolin that affect only the rate of G_s or G_i activation would have no effect on the reference experimental condition (forskolin alone). Alternatively, experimental perturbations that effect only the equilibrium constants would alter both the reference time courses (forskolin alone) and the time course obtained with Gpp(NH)p and forskolin, and the magnitude of the alteration would depend on the exact initial concentrations of each of the active and inactive species of adenylate cyclase. This type of logic will be used below to interpret data obtained with pertussis toxin and phorbol ester as perturbants.

The simulations of Fig. 3 also demonstrate a point important in the interpretation of experimental time courses obtained with nonhydrolyzable guanine nucleotides for dual-regulated systems such as adenylate cyclase. Frequently, such time

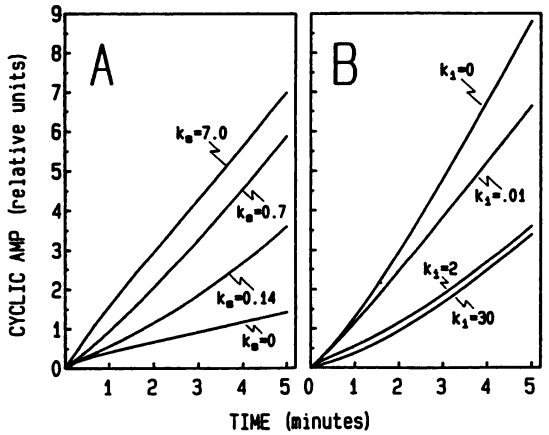

Fig. 2. Simulations of the effect of k_s and k_i. Theoretical curves were generated using Eq. 5 (model I) with the parameters described in Fig. 1A, with the following variations. A, k_s was varied: 0/min, 0.14/min, 0.7/min, and 7.0/min. B, k_i was varied: 0/min, 0.01/min, 2.0/min, and 30.0/min. Comparable results are obtained using model II.

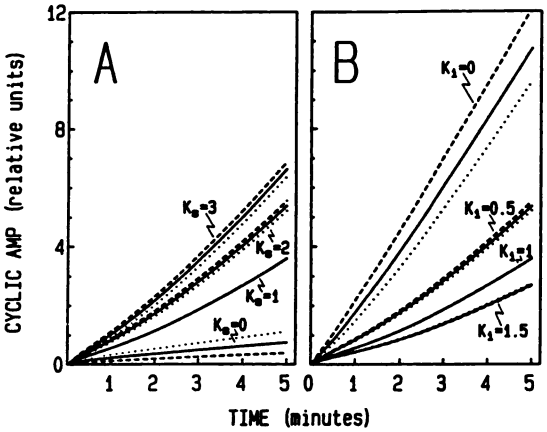

Fig. 3. Simulations of the effect of K_s and K_i. Theoretical curves were generated using Eq. 5 (model I) with the parameters described in Fig. 1A with the following variations. A, To simulate relative changes in K_s of 0, 1, 2, and 3 (1 corresponding to the relative value of K_s that simulates the data in Fig. 1A), the values of $K_sG_{s_0}^*$ and $K_sG_{s_0}$ were 0, 0; 1.0, 16.71; 2.0, 33.4; and 3.0, 50.1, respectively (——). To simulate the effect of changing the initial state, $K_iG_{i_0}^*$ and $K_iG_{i_0}$ were set at 3.0 and 18.75 (high initial concentration of G_i^*) (– – –) or 0.3 and 6.1 (low initial concentration of G_i^*) (· · · ·). Applying the methodology described in the text (Eqs. 12–15), the corresponding values of $K_sG_{s_0}^*$ and $K_sG_{s_0}$ for relative changes in K_s of 0, 1, 2, and 3 were 0, 0; 3.02, 33.5; 6.04, 67.0; and 9.06, 100.5 (– – –) and 0, 0; 0.31, 10.89; 0.62, 21.8; and 0.94, 32.7 (· · · ·). B, The values of $K_iG_{i_0}^*$ and $K_iG_{i_0}$ were varied to simulate relative changes in K_i of 0, 0.5, 1.0, and 1.5 (1.0 corresponding to the relative value of K_i simulating the data of Fig. 1A), as described for A, at the same initial conditions of Fig. 1A (——) or at high initial G_i^* (– – –) or low initial G_i^* (· · · ·). The values of $K_iG_{i_0}^*$ and $K_iG_{i_0}$ were 0, 0; 0.5, 4.68, 1.0, 9.36; and 1.5, 14.04 (——); 0, 0; 1.5, 9.38; 3.0, 18.75; and 4.5, 28.13 (– – –); and 0, 0; 0.15, 3.05; 0.3, 6.1; and 0.45, 9.15 (· · · ·) for relative values of K_i equal to 0, 0.5, 1.0, and 1.5, respectively. $K_sG_{s_0}^*$ and $K_sG_{s_0}$ were 1.0 and 16.71 (——); 3.02 and 33.5 (– – –); and 0.31 and 10.89 (· · · ·).

courses have been interpreted by estimating "lag times" for the onset of apparent steady state activity. These lag times have generally been obtained by extrapolation from the linear portion of the time course to the abscissa or some other reference (see Refs. 9, 10, 15, and 17, for example). Perturbations that affect these lag times have been interpreted to mean that the rates of activation of G_s or G_i have been affected. Although such an interpretation may sometimes be valid, Fig. 4 demonstrates that perturbations of the equilibria between the components of adenylate cyclase will also alter the lag times, even though the rate constants k_s and k_i remain unchanged. Thus, one must use caution when interpreting complex time course data from estimates of lag times. Using a quantitative model for analysis is superior, because the entire time course is considered and contributions of changes in equilibrium constants to the time dependence are included.

Effect of pertussis toxin. Experimentally, long term treatment with pertussis toxin decreased the forskolin-stimulated adenylate cyclase activity in the absence of Gpp(NH)p from an average of 378 pmol/min/mg to 283 pmol/min/mg. This corresponds to a 25% reduction in either k_cA_T or the proportion of A_1 species to A_0 species. Taking the reference condition (forskolin alone, no pertussis toxin treatment) as having an activity of 1.0 unit/min, as described above, the activity with forskolin alone after pertussis toxin treatment is obtained either by reducing k_cA_T from 2.8 units/min to 2.1 units/min or by reducing K_o from 0.56 to 0.37 in model I or from 0.01 to 0.0066 in model II. In contrast to the reduction in the reference (forskolin-stimulated) activity, the amount of cAMP produced upon inclusion of Gpp(NH)p was greater with pertussis toxin treatment than without (Fig. 5A). Therefore, a second, apparently stimulatory, effect of pertussis toxin was also present. We assumed that this second effect was the reduction in the rate of activation of G_i (k_i) suggested previously (17) and presumably due to the ADP-ribosylation of the α subunit by the toxin (18).

We, thus, simulated the data obtained with forskolin and Gpp(NH)p with or without pertussis toxin treatment using model I (Fig. 5A). All model parameters were invariant between simulations of control and pertussis toxin data, except for k_i and either k_cA_T or K_o. The data were reproduced equally well if k_cA_T was set at 2.1 units/min with k_i at 0.011/min [control value (no pertussis toxin) equals 2.0/min] or if K_o was set at 0.37 and k_i was set at 0.028/min. The curve for pertussis toxin in Fig. 5A is the simulation with k_cA_T equal to 2.1 units/min. The ability of the computer simulations to reproduce the data with variations in these parameters is independent of which model is used. Fig. 5B demonstrates the same data simulated with model II (Eqs. 6 and 7) instead of model I.

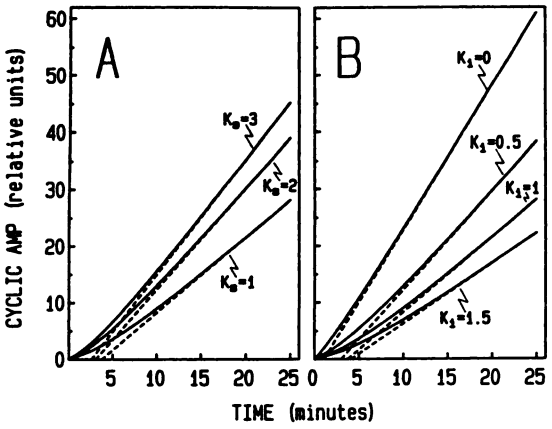

Fig. 4. Effect of K_s and K_i on the lag time. ——, The theoretical curves were generated exactly as for the *solid curves* in Fig. 3. Lag times are represented by linear extrapolation of the last three points of each curve to the *abscissa* (– – –).

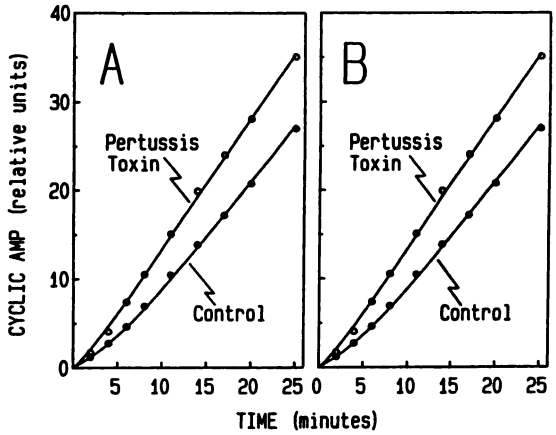

Fig. 5. Comparison of computer simulations with the experimental effect of pertussis toxin on forskolin/Gpp(NH)p-stimulated cAMP production. Membranes from cells treated 24 hr without (●) or with (○) 100 ng/ml pertussis toxin were assayed for adenylate cyclase activity in the presence of 50 μM forskolin and 10 μM Gpp(NH)p, as described in Experimental Procedures. Data are means of three experiments and are normalized to the time courses obtained without Gpp(NH)p or pertussis toxin (2-min point, 343 ± 61 pmol/min/mg; all other points, 378 ± 50 pmol/min/mg). A, Theoretical curves were generated with Eq. 5 (model 1). The parameters for the control data were k_cA_T = 2.8 units/min, $K_sG_{s_0}{}^*$ = 1.0, $K_sG_{s_0}$ = 13.5, $K_iG_{i_0}{}^*$ = 1.0, $K_iG_{i_0}$ = 8.0, K_o = 0.56, k_i = 2.0/min, and k_s = 0.14/min. The same parameters were used for the pertussis toxin curve, with the exception that k_cA_T = 2.1 units/min and k_i = 0.011/min. B, Theoretical curves were generated with model II, using Eqs. 6 and 7, and the parameters for the control curve were k_cA_T = 2.8 units/min, $K_sG_{s_0}{}^*$ = 110, $K_sG_{s_0}$ = 758, $K_{i_s}G_{i_0}{}^*$ = 1.0, $K_{i_s}G_{i_0}$ = 8.14, K_o = 0.01, k_i = 2.0/min, k_s = 0.14/min. The pertussis toxin curve was identical except that k_cA_T = 2.1 units/min and k_i = 0.011/min.

The results of our simulation of the pertussis toxin data are not especially surprising, and it should be emphasized that they only show that the hypothesis previously suggested (17) is consistent with the data. The data could also have been reasonably simulated by letting $K_iG_{i_0}$ = 0. The most important result of this successful simulation is that it provides an estimate of λ_4 for the calculation of model parameters.

The decrease in the reference activity after prolonged pertussis toxin treatment (>18 hr) has been reported previously for S49 cells but without interpretation (19, 20). It may relate to a recent study by Watkins *et al.* (21) suggesting that 24-hr exposure of S49 cells to pertussis toxin results in a decrease in the cellular concentration of some of the components of adenylate cyclase and appears to be unrelated to the ADP-ribosylation of the α subunit of G_i. Presumably, one could use the experimental and analytical approach described here to examine the relative effects of ADP-ribosylation and selective protein depletion on the time course of adenylate cyclase regulation in cell membranes by varying the length of the pertussis toxin treatment and correlating the effects on the time courses with changes in protein concentrations and amounts of ADP-ribosylation, as described by Watkins *et al.* (21).

Effect of phorbol esters. In a variety of cells, phorbol ester treatment enhances the production of cAMP stimulated by

forskolin, guanine nuclotide, and other reagents (10, 22–27). This effect has been attributed to the phosphorylation of either G_i (23) or the catalytic subunit of adenylate cyclase (25) by phorbol ester-activated protein kinase C (28). In S49 cells and platelets, a variety of data have suggested that the effect of phorbol ester treatment is largely due to an attenuation of the G_i-mediated inhibition of adenylate cyclase (10, 22, 23) and may be qualitatively similar to the effect of pertussis toxin (10, 22). However, we have been unable, using column chromatography, immunoblotting, and electrophoresis, to obtain convincing evidence of *in vivo* phosphorylation of G_i upon TPA treatment in S49 cells.[1] Furthermore, recent evidence reported by Carlson *et al.* (29) indicates that the GTP-binding protein phosphorylated by protein kinase C *in vivo* is not G_i. The question we have asked, then, is whether it is possible to reconcile quantitatively the effect of phorbol ester in S49 cell membranes as being an effect (presumably phosphorylation) on the catalytic subunit of adenylate cyclase even with a model that does not include a direct interaction between the catalytic subunit of adenylate cyclase and G_i (i.e., model II).

Experimentally, TPA treatment enhanced the rate of forskolin-stimulated cAMP accumulation in the absence of Gpp(NH)p by 33%, which was similar to previous findings (10, 22). TPA increased the initial rate of cAMP generation in the presence of Gpp(NH)p by about 50% and enhanced the maximum rate about 20% (Fig. 6A). This differential effect of TPA treatment on the initial rate relative to the final rate in the time courses is one type of evidence interpreted previously as a reduction in G_i-mediated inhibition of adenylate cyclase (10)[2].

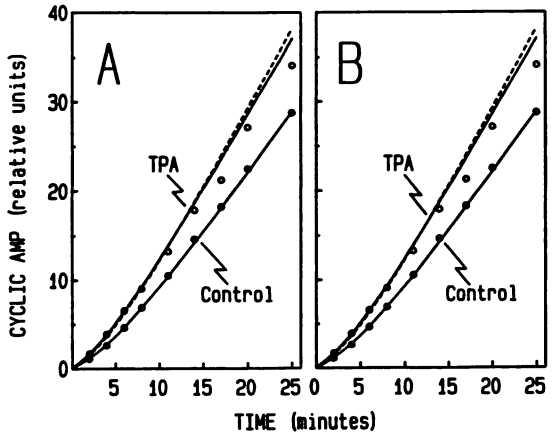

Fig. 6. Effect of TPA on the time course of Gpp(NH)p modulation of forskolin-stimulated cAMP production. Membranes from cells treated 10 min with (○) or without (●) 100 nM TPA were assayed for adenylate cyclase activity with 50 μM forskolin and 10 μM Gpp(NH)p, as described in Experimental Procedures. Data are means of three separate experiments and are normalized to the time courses obtained without Gpp(NH)p or TPA treatment (2 min point, 285 ± 53 pmol/min/mg; all other points, 320 ± 101 pmol/min/mg). A, Theoretical curves were generated using Eq. 5 (model I). The parameter values for control were $k_cA_T = 2.8$ units/min, $K_sG_{s_0}{}^* = 1.0$, $K_sG_{s_0} = 20.7$, $K_iG_{i_0}{}^* = 1.0$, $K_iG_{i_0} = 11.0$, $K_o = 0.56$, $k_i = 2.0$/min, $k_s = 0.14$/min. For TPA curves, the parameter values were identical except for the following: hypothesis 1 (– – –), $k_cA_T = 3.7$ units/min; hypothesis 2 (——), $K_o = 0.91$. B, Theoretical curves were generated using Eqs. 6 and 7 (model II). Control parameter values were $k_cA_T = 2.8$ units/min, $K_sG_{s_0}{}^* = 110$, $K_sG_{s_0} = 1162$, $K_{i_s}G_{i_0}{}^* = 1.0$, $K_{i_s}G_{i_0} = 11.19$, $K_o = 0.01$, $k_i = 2.0$/min, $k_s = 0.14$/min. The parameters for the TPA curve were identical except for the following: Hypothesis 1 (– – –), $k_cA_T = 3.7$ units/min; hypothesis 2 (——), $K_o = 0.0163$.

The general model used in this report allows two ways in which the activity of the catalytic subunit could hypothetically be altered by protein kinase C. 1) The intrinsic activity of the active form of the enzyme could be increased. This is equivalent to increasing the value of k_cA_T in the model. 2) Phorbol ester-activated protein kinase C could alter the equilibrium between active and inactive adenylate cyclase. This effect is simulated equivalently by increasing K_s or K_o, or by decreasing K_i. For simplicity, we increased K_o because it required alteration of only one parameter in the simulations. The fact that phorbol ester treatment increased the activity of the reference state (forskolin alone) by a factor of 1.33 ± 0.06 (mean ± SE) fixes the values that must be assigned to k_cA_T or K_o in the simulations (k_cA_T must be increased from 2.8 to 3.7 units/min or K_o must be increased from 0.56 to 0.91 in model I or from 0.01 to 0.0163 in model II). These parameter values were used in simulations of time courses in the presence of forskolin and Gpp(NH)p to test the two hypotheses of the effect of TPA, rather than obtaining a "best fit" by independent parameter variation.

The curves in Fig. 6A are the simulations of these two hypotheses for the effect of phorbol ester treatment on the catalytic subunit using model I. The *solid curve* intersecting the *closed circles* is a simulation of the control data obtained with forskolin plus Gpp(NH)p without TPA treatment, using constants derived as described in Eqs. 12–15. The *dashed curve* intersecting the *open circles* (plus TPA) is a simulation of hypothesis 1, using the same parameter values as the control curve except that the value of k_cA_T was set at 3.7 units/min. The *solid curve* intersecting the *open circles* is a simulation of hypothesis 2, with K_o as the altered parameter (0.91). Both curves reproduced the effect of TPA treatment, although the curves deviated somewhat from the final experimental points in the time course. However, these deviations were small, given the error in the data and in the estimates of the values of the model parameters. For example, a 20% variation in the value of k_s can completely account for the deviation between the simulated curves and the data. Hypothesis 2 seems to simulate the data slightly better, but the difference between the two hypotheses with these data is well within the experimental error. Regardless, it appears that a putative effect of protein kinase C on the catalytic subunit can quantitatively account for the effect of phorbol ester on S49 cell adenylate cyclase.

This conclusion may seem intuitively obvious for a model that includes a direct interaction between G_i and the catalytic subunit. The more important question is whether this effect of phorbol ester to apparently attenuate G_i-mediated inhibition could be reconciled with an effect on the catalytic subunit in a

[1] J. D. Bell and L. L. Brunton, unpublished observations.

[2] As we prepared the present manuscript, we reexamined Ref. 10 and found that we had incorrectly formulated Eq. 6, which should read

$$\frac{dA_i}{dt} = V(1 - e^{-k_s t}) - (V - I)(1 - e^{-k_i t})$$

Thus, Eq. 7 (in Ref. 10) becomes

$$A_i = \frac{(V - I)}{k_i}(1 - e^{-k_i t}) - \frac{V}{k_s}(1 - e^{-k_s t}) + (I)(t)$$

This minor reformulation does not alter the conclusion reached in Ref. 10. Now, when the equation constants are fit to the data, the internal consistency of the data and extracted values are even better; TPA treatment reduces k_i from 0.59/min to 0.22/min (instead of 2.07/min to 0.24/min in the original paper), in better agreement with the apparent change in lag time (1.5 min to 4 min).

model that does not allow for a direct interaction between the catalyst and G_i (i.e., model II). Fig. 6B represents simulations of the data using model II with identical perturbations of k_cA_T (Fig. 6B, *dashed curve*) or K_o (Fig. 6B, *upper solid curve*). The results are equivalent to those obtained with model I. Thus, the effect of phorbol ester can be described by an effect on only the catalytic subunit, regardless of the mechanism of G_i-mediated inhibition, if the proportion of active to inactive forms is coupled by a reversible equilibrium.

Some of the more convincing previous evidence that the effect of phorbol ester involves a reduction in adenylate cyclase inhibition by G_i was obtained from cyc$^-$ S49 cells, which lack the α subunit of G_s (1) and with which only inhibition of forskolin-stimulated adenylate cyclase is seen upon addition of Gpp(NH)p (10, 17). In an attempt to better discover whether the hypotheses for effects of the phorbol ester on the catalytic subunit can quantitatively reproduce the effect of TPA on adenylate cyclase, we re-examined experimental time courses obtained with forskolin and Gpp(NH)p in the cyc$^-$ S49 cell from a previous study (10). $K_sG_{s_0}{}^*$ and $K_sG_{s_0}$ were set equal to zero in simulations of Eq. 5, because cyc$^-$ cells lack G_s. The same values of k_cA_T and K_o were used as for the wild-type cells. The value of $K_iG_{i_0}{}^*$ was necessarily adjusted (because of the lack of G_s) to give the normalized reference activity of 1.0 unit/min:

$$\frac{dcAMP}{dt} = \frac{k_cA_TK_o}{1 + K_iG_{i_0}{}^* + K_o} = 1.0\ unit/min \qquad (16)$$

As for the simulations of data with wild-type cells (Figs. 1–6) using model I, the selection of the inital values of K_o or $K_iG_{i_0}{}^*$ was unimportant, as long as the conditions of Eq. 16 were met. The value of $K_iG_{i_0}$ was calculated using Eq. 5 and the final slope of the control data from Fig. 7 (0.27 units/min). The rate constant k_i was adjusted to optimally produce the complete time dependence. Fig. 7 demonstrates that the model can reproduce effectively time course data from the cyc$^-$ membranes stimulated with forskolin and Gpp(NH)p (control).

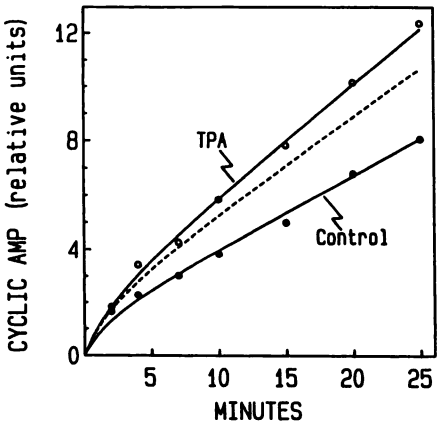

Fig. 7. Simulation of the effect of TPA on cyc$^-$ adenylate cyclase. The experimental data represent the same data of Fig. 6B of Ref. 10. Cyc$^-$ S49 cells were treated without (●) or with (○) 100 nM TPA. Membranes were assayed for adenylate cyclase activity as described in Experimental Procedures, in the presence of 100 μM Gpp(NH)p. Data are the means of three separate experiments, each normalized to the adenylate cyclase activity measured in the presence of forskolin alone (30.8 ± 3.0 pmol/min/mg). The control theoretical curve was generated from Eq. 5 (model I) with $K_sG_{s_0}{}^*$ and $K_sG_{s_0}$ fixed at zero. The values of the variable parameters were k_cA_T = 2.8 units/min, $K_iG_{i_0}{}^*$ = 0, $K_iG_{i_0}$ = 4.25, K_o = 0.56, k_i = 0.27/min. Parameter values for the TPA curves were identical except: hypothesis 1 (– – –), k_cA_T = 3.7 units/min; hypothesis 2 (——), K_o = 0.91.

The result of TPA treatment on the time course of Gpp(NH)p- and forskolin-stimulated adenylate cyclase in Cyc$^-$ S49 cells is shown by the *open circles* in Fig. 7. The relative increase in the reference activity after TPA treatment was identical in the cyc$^-$ cells, compared with the wild-type cells (1.32 ± 0.04 units/min). Therefore, the numerical values used for k_cA_T and K_o with TPA-treated wild-type cells were also appropriate for cyc$^-$ cells. Thus, to test these hypotheses for the effect of the phorbol ester, we again increased either k_cA_T to 3.7 units/min or K_o to 0.91. As shown by the *upper curves* in Fig. 7, both hypotheses qualitatively simulated the data. However, quantitative differences were more apparent between the two hypotheses in cyc$^-$ membranes than in wild-type membranes. The simulated time course with hypothesis 1 (k_cA_T; Fig. 7, *dashed lines*) clearly underestimates the amount of cAMP produced after TPA treatment. This means that hypothesis 1 does not reconcile the apparent reduction in G_i-mediated inhibition. The best agreement with the data was again obtained with hypothesis 2 (Fig. 7, *solid curves*).

Of course, the data of Fig. 6 and 7 would be reproduced equally well by varying multiple parameters in the model. More complex mechanisms are always possible and are difficult to rule out. The data and simulations shown here simply demonstrate that the hypothesis that the complex effects of phorbol ester to enhance adenylate cyclase activity and reduce the apparent inhibition by G_i could be due to a single perturbation of the catalytic subunit is quantitatively viable. Furthermore, we have shown that such is true regardless of the mechanism of G_i-mediated inhibition. This analysis is especially important in light of increasing evidence that G_i may not be significantly phosphorylated by protein kinase C *in vivo* (29).[1]

Analysis of the effect of forskolin. Throughout this report we have used 50 μM forskolin as the experimental condition for the initial or reference state. This concentration of forskolin was carefully chosen in preliminary experiments to give time courses of cAMP production in the presence of Gpp(NH)p that would display both inhibition and stimulation of the reference activity. Indeed, Hudson and Fain (8) showed that the shape of the time course upon addition of nonhydrolyzable guanine nucleotide depends very much upon the amount of forskolin used in the experiment. Their results are as follows. At low concentrations of forskolin, only a time-dependent stimulation of adenylate cyclase activity is seen when Gpp(NH)p is included; the time course only curves upward from the reference time course. At intermediate concentrations, data such as those presented in this report are obtained; the rate of cAMP production first decreases and then begins to increase until achieving a maximal rate greater than that found in the absence of Gpp(NH)p. At high concentrations of forskolin, the inhibitory phase of the time course with Gpp(NH)p is more pronounced than at lower concentrations, and the rate of cAMP production eventually begins to increase until it reaches a value equal to the maximum value obtained in the absence of guanine nucleotide.

It has been reported from a number of sources that forskolin activates the isolated catalytic subunit of adenylate cyclase (reviewed in Ref. 13). Therefore, forskolin must affect the value of either k_cA_T or K_o in the models presented here. For example, if forskolin binds only to the active state of the catalytic

subunit, then it would increase the apparent value of K_o. However, a change in either of these two parameters cannot account for the changes in the shapes of the time courses in the presence of Gpp(NH)p reported by Hudson and Fain (8) as a function of forskolin concentration. First, inspection of either Eq. 5 (model I) or Eq. 6 (model II) immediately reveals that variation of k_cA_T only affects the amount of cAMP produced and cannot change the shape of a time course. Second, we demonstrate in the Appendix to this report that K_o, although it can affect the shape of the time courses, cannot be varied in a manner to produce time courses that exhibit initial stimulation at certain values of K_o and exhibit initial inhibition at other values. Therefore, any rationalization of the qualitative features of the data reported by Hudson and Fain (8) must involve the coupling of the GTP-binding proteins, and this requires introduction of (an) additional parameter(s) into the model.

The conditions under which the two models will produce time courses in which either inhibition or stimulation is observed at zero time are derived in the Appendix. For initial stimulation to occur, the following criteria must be met

$$\text{Model I: } k_sK_sG_{s_0} > \frac{(1 + K_sG_{s_0}^*)}{(1 + K_iG_{i_0}^*)}k_iK_iG_{i_0} \qquad (17a)$$

$$\text{Model II: } k_sG_{s_0} > \frac{K_{is}G_{s_0}^*}{(1 + K_{is}G_{i_0}^*)}k_iG_{i_0} \qquad (17b)$$

Because $k_i > k_s$ and because the concentration of G_i is probably greater than that of G_s (1), either $G_{i_0}^*$ must be relatively large or $G_{s_0}^*$ must be relatively small for the time course to be purely stimulatory in the presence of Gpp(NH)p. The criteria for initial inhibition to occur are the converse. Therefore, $G_{i_0}^*$ must be small or $G_{s_0}^*$ must be large. Given the existing data with forskolin (13), a logical interpretation of the Hudson and Fain results is that forskolin affects the value of $K_sG_{s_0}^*$.

We have, thus, simulated the qualitative result obtained by Hudson and Fain (8), using model I and varying $G_{s_0}^*$ (Fig. 8). These simulations required the calculation of a new set of

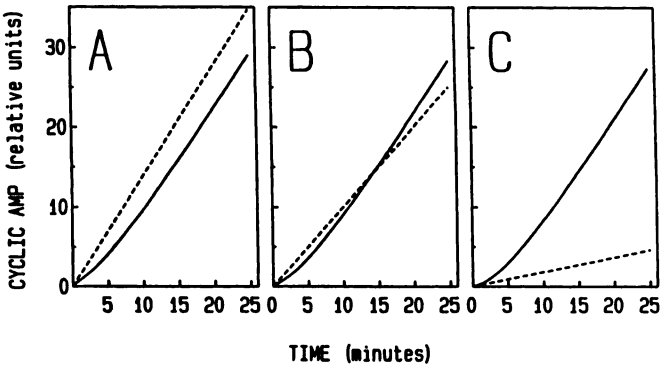

Fig. 8. Simulations of the effect of $G_{s_0}^*$. Theoretical curves were generated by numerical integration of Eq. 5 (model I). – – –, Forskolin alone (k_s and k_i = 0); ——, forskolin plus Gpp(NH)p throughout. Constant parameters were calculated according to Eqs. 12–15 and were k_cA_T = 2.8 units/min, k_i = 2.0/min, k_s = 0.14/min, $K_iG_{i_0}^*$ = 7.0, $K_iG_{i_0}$ = 36.9, and K_o = 0.56. To simulate the effect of forskolin concentration as an effect on the value of $G_{s_0}^*$, we varied the values of both $K_sG_{s_0}^*$ and $K_sG_{s_0}$ because the total amount of G_s must be conserved (i.e., $K_sG_{s_0}^* + K_sG_{s_0}$ = constant). A (high concentration of forskolin), $K_sG_{s_0}^*$ = 13.0 and $K_sG_{s_0}$ = 60.6. B intermediate concentration of forskolin, $K_sG_{s_0}^*$ = 6.94 and $K_sG_{s_0}$ = 66.7. C (low forskolin concentration), $K_sG_{s_0}^*$ = 0.1 and $K_sG_{s_0}$ = 73.5.

equilibrium constants for the model, due to the constraints of Eq. 17a. As we have already stated, the data in Figs. 1 and 5 do not provide sufficient information for assignment of specific values for $K_iG_{i_0}^*$, $K_sG_{s_0}^*$, and K_o. Hence, values for two of the three parameters were selected arbitrarily and the third was calculated from Eqs. 12–15. Now, the qualitative result of Hudson and Fain places one additional constraint upon the models. Consequently, for any value of K_o and calculating the other parameters according to Eqs. 12–15, the inequality of Eq. 17a can only be satisfied with certain values of $K_iG_{i_0}^*$ (e.g., if K_o = 0.56 and because $K_sG_{s_0}^* \geq 0$, $K_iG_{i_0}^* \geq 7$).

We have not attempted to quantitatively analyze the data of Hudson and Fain. It should be noted that the limiting rates of cAMP formation measured by Fain and Hudson are a function of the forskolin concentration, whereas they are essentially identical in the simulated data (Fig. 8). In order to reproduce this aspect of the time courses, we would have to vary an additional parameter in the model, such as K_cA_T or K_o, as a function of forskolin concentration. The experimental precedence to justify such a manipulation already exists as stated above (13). A unified hypothesis that would satisfy both the qualitative and quantitative results of Hudson and Fain is that forskolin can form a complex with A_1 and a ternary complex with G_s^* and A_1. Such an effect of forskolin would increase the apparent values of K_o and $K_sG_{s_0}^*$.

Formation of such a ternary complex, then, is a unified working hypothesis for the effect of forskolin. These results suggest some future directions to pursue with this approach. First, the hypothesis for the effect of forskolin can be explicitly incorporated into the models. Measurement of the apparent binding of forskolin to the membranes as a function of forskolin concentration, with and without nonhydrolyzable guanine nucleotide, in wild-type and cyc$^-$ membranes will estimate the strength of the interaction of forskolin with the different states of the system. If the models of adenylate cyclase regulation and the hypothesis for forskolin are correct, one should be able to simulate quantitatively time courses of cAMP production with and without Gpp(NH)p, at various concentrations of forskolin, using K_o and $G_{s_0}^*$ as the only variables and with values that are self-consistent with the binding data. Also shown in Fig. 8 and Eqs. 17a and 17b, the added dimension of varying the forskolin concentration with and without the Gpp(NH)p constrains the values of $K_iG_{i_0}^*$ and $K_sG_{s_0}^*$, which in turn constrain the value of K_o, based on Eqs. 12–15. The value of K_o as a function of forskolin concentration could also be estimated using cyc$^-$ membranes, because G_s^* would not be present (1). Furthermore, Eq. 17b indicates that an independent estimate of the relative functional amounts of activatable G_s and G_i would help constrain parameter values for model II. Such an estimate could presumably be obtained using ADP-ribosylation by bacterial toxins (1) or using antibodies (30). Together, these approaches should provide substantial information regarding the initial or reference state of the system. As discussed above (Fig. 1B), this information is important for judging the viability of the models.

Appendix: Condition for Initial Inhibition/ Stimulation of Adenylate Cyclase Activity in the Presence of Guanine Nucleotides

An important distinction between various time courses of adenylate cyclase activity is whether the initial activity is inhibited or stimulated in the presence of guanine nucleotide

(see Fig. 8 and discussion in the text). Although it is commonly accepted that such inhibition is the result of rapid activation of the inhibitory GTP-binding protein system, the conditions necessary to observe such inhibition have not been explicitly defined in terms of a mechanistic model for the reaction scheme. In this Appendix, we derive the conditions for the two models of inhibition/activation discussed in the main body of this paper.

Model I: Inhibition by direct interaction of G_i* with the catalytic subunit. In this model, the normalized rate of cAMP production is given by

$$r(t) = \frac{dcAMP/dt}{k_c A_T} = \frac{K_o(1 + K_s G_s^*)}{1 + K_i G_i^* + K_o(1 + K_s G_s^*)} \quad (A1)$$

Assuming that only G_s* and G_i* vary with time, it follows that

$$\frac{dr(t)}{dt} = \frac{K_o[K_s(1 + K_i G_i^*)\frac{dG_s}{dt} - K_i(1 + K_s G_s^*)\frac{dG_i^*}{dt}]}{[1 + K_i G_i^* + K_o(1 + K_s G_s^*)]^2} \quad (A2)$$

The condition for inhibition is $d(r(t))/dt < 0$. Therefore, if inhibition is to occur,

$$K_i(1 + K_s G_s^*)\frac{dG_i^*}{dt} > K_s(1 + K_i G_i^*)\frac{dG_s^*}{dt} \quad (A3)$$

For model I, G* (t) and G_i* (t) are given by Eqs. 3 and 4 in the text. Thus,

$$\frac{dG_i^*}{dt} = k_i G_{i_0} e^{-k_i t} \quad (A4a)$$

$$\frac{dG_s^*}{dt} = k_s G_{s_0} e^{-k_s t} \quad (A4b)$$

Therefore, at $t = 0$

$$K_i(1 + K_s G_{s_0}^*) k_i G_{i_0} > K_s(1 + K_i G_{i_0}^*) k_s G_{s_0} \quad (A5)$$

if initial inhibition is to be observed.

Model II: Direct interaction between G_i* and G_s*. In this model,

$$r(t) = \frac{K_o(1 + K_s G_s^*)}{1 + K_o(1 + K_s G_s^*)} \quad (A6)$$

and

$$\frac{dr(t)}{dt} = \frac{K_o K_s \frac{dG_s^*}{dt}}{[1 + K_o(1 + K_s G_s^*)]^2} \quad (A7)$$

Inhibition will be observed only if $dG_s^*/dt < 0$. Assuming that G_s* is given by

$$G_s^* = \frac{G_{s_0}^* + G_{s_0}(1 - e^{-k_s t})}{1 + K_{i_s} G_{i_0}^* + K_{i_s} G_{i_0}(1 - e^{-k_i t})} \quad (A8)$$

it follows that at $t = 0$

$$\frac{dG_s^*}{dt} = \frac{k_s G_{s_0}(1 + K_{i_s} G_{i_0}^*) - G_{s_0}^* k_i K_{i_s} G_{i_0}}{(1 + K_{i_s} G_{i_0}^*)^2} \quad (A9)$$

Therefore, initial inhibition will be observed if

$$k_s G_{s_0} < \frac{k_i K_{i_s} G_{i_0} G_{s_0}^*}{1 + K_{i_s} G_{i_0}^*} \quad (A10)$$

It should be noted that the conditions for initial stimulation are the converse of those given in Eqs. A5 and A10 for inhibition.These results demonstrate two important conclusions derived from the two models. 1) From Eqs. A5 and A10, it follows that observation of initial inhibition or activation relative to the reference state is independent of both K_o and $k_c A_T$. 2) For initial inhibition to be observed with model II, the system must be at least partially activated by G_s at zero time (i.e., $G_{s_0}^* \neq 0$). For model I, only the potential for inhibition ($G_{i_0} \neq 0$) is required. Although these conditions are necessary for initial inhibition in the two models, they are not sufficient. Thus, for the adenylate cyclase system to be switched from initial activation to initial inhibition by some perturbant such as forskolin, it is necessary that model parameters associated with interactions involving one or both of the GTP-binding proteins be altered. This does not mean, however, that the apparent values of parameters such as K_o could not also be affected by the perturbant.

References

1. Gilman, A. G. G proteins: transducers of receptor-generated signals. *Annu. Rev. Biochem.* **56**:615–649 (1978).
2. Katada, T., G. M. Bokoch, M. D. Smigel, M. Ui, and A. G. Gilman. The inhibitory guanine nucleotide-binding regulatory component of adenylate cyclase: subunit dissociation and the inhibition of adenylate cyclase in S49 lymphoma cyc⁻ and wild type membranes. *J. Biol. Chem.* **259**:3586–3595 (1984).
3. Hildebrandt, J. D., J. Codina, and L. Birnbaumer. Interaction of the stimulatory and inhibitory regulatory proteins of the adenylyl cyclase system with the catalytic component of cyc⁻ S49 cell membranes. *J. Biol. Chem.* **259**:13178–13185 (1984).
4. Katada, T., M. Oinuma, and M. Ui. Mechanisms for inhibition of the catalytic activity of adenylate cyclase by the guanine nucleotide-binding proteins serving as the substrate of islet-activating protein, pertussis toxin. *J. Biol. Chem.* **261**:5215–5221 (1986).
5. Enomoto, K., and T. Asakawa. Inhibition of catalytic unit of adenylate cyclase and activation of GTPase of N_i protein by $\beta\gamma$-subunits of GTP-binding proteins. *FEBS Lett.* **202**:63–68 (1986).
6. Katada, T., J. K. Northrup, G. M. Bokoch, M. Ui, and A. G. Gilman. The inhibitory guanine-nucleotide-binding regulatory component of adenylate cyclase: subunit dissociation and guanine nucleotide-dependent hormonal inhibition. *J. Biol. Chem.* **259**:3578–3585 (1984).
7. Cerione, R. A., C. Staniszewski, P. Gierschik, J. Codina, R. L. Somers, L. Birnbaumer, A. M. Spiegel, M. G. Caron, and R. J. Lefkowitz. Mechanism of guanine nucleotide regulatory protein-mediated inhibition of adenylate cyclase. *J. Biol. Chem.* **261**:9514–9520 (1986).
8. Hudson, T. H., and J. N. Fain. Forskolin-activated adenylate cyclase: inhibition by guanyl-5-yl imidodiphosphate. *J. Biol. Chem.* **258**:9755–9761 (1983).
9. Bell, J. D., I. L. O. Buxton, and L. L. Brunton. Enhancement of adenylate cyclase activity in S49 lymphoma cells by phorbol ester: putative effect of C kinase on α_s-GTP-catalytic subunit interaction. *J. Biol. Chem.* **260**:2625–2628 (1985).
10. Bell, J. D., and L. L. Brunton. Enhancement of adenylate cyclase activity in S49 lymphoma cells by phorbol esters: withdrawal of GTP-dependent inhibition. *J. Biol. Chem.* **261**:12036–12041 (1986).
11. Bradford, M. M. A rapid and sensitive method for the quantitation of microgram quantities of protein utilizing the principle of protein-dye binding. *Anal. Biochem.* **72**:248–254 (1976).
12. Salomon, Y., C. Londos, and M. Rodbell. A highly sensitive adenylate cyclase assay. *Anal. Biochem.* **58**:541–548 (1974).
13. Seamon, K. B., and J. W. Daly. Forskolin: its biological and chemical properties. *Adv. Cyclic Nucleotide Protein Phosphorylation Res.* **20**:1–150 (1986).
14. Strittmatter, S., and E. J. Neer. Properties of the separated catalytic and regulatory units of brain adenylate cyclase. *Proc. Natl. Acad. Sci. USA* **77**:6344–6348 (1980).
15. Wong, S. K.-F., and B. R. Martin. The interactions between the activatory guanine nucleotide binding protein and the catalytic subunit of adenylate cyclase in rat liver plasma membranes. *Biochem. J.* **231**:39–46 (1985).
16. Levitski, A. Regulation of adenylate cyclase by hormones and G-proteins. *FEBS Lett.* **211**:113–118 (1987).
17. Jakobs, K. H., K. Aktories, and G. Schultz. Mechanism of pertussis toxin action on the adenylate cyclase system: inhibition of the turn-on reaction of the inhibitory regulatory site. *Eur. J. Biochem.* **140**:177–181 (1984).
18. Murayama, T., and M. Ui. Loss of the inhibitory function of the guanine nucleotide regulatory component of adenylate cyclase due to its ADP-ribo-

sylation by islet-activating protein, pertussis toxin, in adipocyte membranes. *J. Biol. Chem.* **258**:3319–3326 (1983).
19. Hewlett, E. L., M. J. Cronin, J. Moss, H. Anderson, G. A. Myers, and R. D. Pearson. Pertussis toxin: lessons from biological and biochemical effects in different cells. *Adv. Cyclic Nucleotide Protein Phosphorylation Res.* **17**:173–182 (1984).
20. Malchoff, C. D., L. Huang, N. Gillespie, C. Villar Palasi, C. F. W. Schwartz, K. Cheng, E. L. Hewlett, and J. Larner. A putative mediator of insulin action which inhibits adenylate cyclase and adenosine 3′5′-monophosphate-dependent protein kinase: partial purification from rat liver: site and kinetic mechanism of action. *Endocrinology* **120**:1327–1337 (1987).
21. Watkins, D. C., J. K. Northup, and C. C. Malbon. Pertussis toxin treatment *in vivo* is associated with a decline in G-protein β-subunits. *J. Biol. Chem.* **264**:4186–4194 (1989).
22. Johnson, J. A., T. J. Goka, and R. B. Clark. Phorbol ester-induced augmentation and inhibition of epinephrine-stimulated adenylate cyclase in S49 lymphoma cells. *J. Cyclic Nucleotide Protein Phosphorylation Res.* **11**:199–215 (1986).
23. Katada, T., A. G. Gilman, Y. Watanabe, S. Bauer, and K. H. Jakobs. Protein kinase C phosphorylates the inhibitory guanine-nucleotide-binding regulatory component and apparently suppresses its function in hormonal inhibition of adenylate cyclase. *Eur. J. Pharmacol.* **151**:431–437 (1985).
24. Langlois, D., J.-M. Saez, and M. Begeot. The potentiating effects of phorbol ester on ACTH-, cholera toxin-, and forskolin-induced cAMP production by cultured bovine adrenal cells is not mediated by the inactivation of α subunit of G_i protein. *Biochem. Biophys. Res. Commun.* **146**:517–523 (1987).
25. Yoshimasa, T., D. R. Sibley, M. Bouvier, R. J. Lefkowitz, and M. G. Caron. Cross-talk between cellular signalling pathways suggested by phorbol-ester-induced adenylate cyclase phosphorylation. *Nature* (*Lond.*) **327**:67–70 (1987).
26. Summers, S. T., J. M. Walker, J. J. Sando, and M. J. Cronin. Phorbol esters increase adenylate cyclase activity and stability in pituitary membranes. *Biochem. Biophys. Res. Commun.* **151**:16–24 (1988).
27. Sibley, D. R., R. A. Jeffs, K. Daniel, P. Nambi, and R. J. Lefkowitz. Phorbol diester treatment promotes enhanced adenylate cyclase activity in frog erythrocytes. *Arch. Biochem. Biophys.* **244**:373–381 (1986).
28. Nishizuka, Y. Studies and perspectives of protein kinase C. *Science* (*Wash. D.C.*) **233**:305–312 (1986).
29. Carlson, K. E., L. F. Brass, and D. R. Manning. Thrombin and phorbol esters cause the selective phosphorylation of a G protein other than G_i in human platelets. *J. Biol. Chem.* **264**:13298–13305 (1989).
30. Ransnas, L. A., and P. A. Insel. Quantitation of the guanine nucleotide binding regulatory protein G_s in S49 cell membranes using antipeptide antibodies to α_s. *J. Biol. Chem.* **263**:9482–9485 (1988).

Send reprint requests to: J. D. Bell, Department of Pharmacology, University of Virginia School of Medicine, Charlottesville, VA 22908.